International Research Journal of Applied Sciences, Engineering and Technology
Vol.8, No. 12, December-2022;
ISSN (1573-1405);
p –ISSN 0920-5691
Impact factor: 4.33

HEAT TRANSFER PERFORMANCE OF A LINEAR FRESNEL SOLAR COLLECTOR ABSORBER TUBES WITH CIRCUMFERENTIAL NON-UNIFORM HEAT FLUX DISTRIBUTIONS

Izuchukwu F. Okafor
National Centre for Energy Research and Development, Africa Centre of Excellence-Sustainable Power and Energy Development University of Nigeria, Nsukka

Abstract: This study investigated the heat transfer performance of a linear Fresnel solar collector absorber tubes with circumferential non-uniform heat flux distributions. A 3D steady-state numerical simulation was implemented on ANSYS Fluent code version 14. The non-uniform solar heat flux distribution was modelled as a sinusoidal function of the concentrated solar heat flux incident on the circumference of the absorber tube. The k-ε model was used to simulate the turbulent flow of the heat transfer fluid through the absorber tube. The tube-wall heat conduction and the convective and irradiative heat losses to the surroundings were also considered in the model. The average internal and axial local transfer coefficients were determined for the sinusoidal circumferential non-uniform heat flux distribution span of 160°, 180°, 200° and 240°, and a 360° span of circumferential uniform heat flux for a 10 m long absorber tubes of a 62 mm inner diameter and a 52 mm wall thickness with thermal conductivity of 16.27 W/mK between the Reynolds number range of 2 600 and 100 000 based on the fluid inlet temperature. The results showed that the average internal heat transfer coefficients for the 360° span of circumferential uniform heat flux with different concentration ratios were approximately the same. The average internal heat transfer coefficient for the absorber tube with uniform heat flux was approximately the same as that of the absorber tubes with the sinusoidal circumferential non-uniform heat flux distributions. The average axial local internal heat transfer coefficient for the uniform heat flux distribution was slightly higher than that of non-uniform flux distributions at the Reynolds number of 4 000. The averaged internal heat transfer coefficient increased with the decrease in the inner diameter of the absorber tube and the wall thickness. However, a decrease in the inner diameter of the tube resulted in an increase in pressure drop and the consequent increase in the pumping power required to overcoming the pressure drop and the turbulent dissipation of the heat transfer fluid. The numerical results showed good agreement with the Nusselt number experimental correlations for fully developed turbulent flow available in the literature.

Key words: absorber tube, solar heat flux, numerical simulation, heat transfer coefficients

1. Introduction

The solar thermal collector systems play very critical role in converting the incident solar irradiation into thermal energy of the heat transfer fluid. In linear Fresnel concentrating solar collector, the solar heat flux impinges on the absorber tubes from the underneath independent of the position of the sun, thereby resulting in circumferential non-uniform heat flux around the tube and hence non-uniform heat transfer to the heat transfer fluid. The previous studies on thermal performance of linear Fresnel concentrating collector absorber tubes were based on uniform solar heat flux, which is not so as revealed in a number of studies. The ray tracing simulation results by Haberle *et al.* [1] showed that the radiation intensity was evenly distributed on the lower part and very low in the upper part of the absorber tube, indicating non-uniform radiation heat flux on the absorber tube. The study also showed that distribution pattern did not vary significantly for different angles of incident solar radiation. The studies by Goswami *et al.* [2] and Mathur *et al.* [3] also showed that flux distribution on the outer-wall surface of the absorber tube had a peak at the central portion from the underneath and decreased rapidly on both sides of the tube. However, the study by Abbas *et al.* [4] on the thermal performance of the linear Fresnel collector receiver tubes of the

International Research Journal of Applied Sciences, Engineering and Technology
Vol.8, No. 12, December-2022;
ISSN (1573-1405);
p –ISSN 0920-5691
Impact factor: 4.33

trapezoidal cavity noted that the solar heat flux impinging on the receiver surface was far from being uniform, but the study assumed a uniform radiation flux impinging on the receiver tube. Experimental validation of an optical and thermal model of a Linear Fresnel Collector by Francisco, *et al*. [5] assumed a uniform radiation flux impinging on the absorber tubes. Other studies which also assumed uniform heat flux include studies by Velázquez *et al.* [6] and Dey [7] etc.

This study numerically investigated the influence of circumferential uniform and non-uniform solar heat flux distributions on the internal and axial local heat transfer coefficients of the absorber tubes of a linear Fresnel concentrating solar collector. The circumferential non-uniform heat flux was modelled as a sinusoidal function of the concentrated solar heat flux incident on the tube. The 3D steady-state numerical simulation of the uniform and non-uniform heat flux distributions on the absorber tube model was implemented on the ANSYS Fluent version 14 [8], which employs finite volume method described in [9]. The tube-wall heat conduction and the convective and irradiative heat losses to the surroundings were also considered in the model. The k-ε model was employed to simulate the turbulent flow of a heat transfer fluid through the absorber tube. The average internal and axial local heat transfer coefficients of a 10 m long absorber tube with a 62 mm inner diameter, a 52 mm wall thickness with a thermal conductivity of 16.27 W/mK are determined with circumferential non-uniform heat flux spans of 160°, 180°, 200° and 240°, and 360° uniform heat flux distributions for the Reynolds number ranging between: 2 600 and 100 000 based on the inlet temperature. The pressure drops and pumping power requirement for four absorber tubes of 10 m long with different inner-wall diameters and thicknesses and their internal heat transfer coefficients were also determined.

2. Physical model description and numerical formulation

The physical model description of the geometry of the tube model used for the numerical simulation of the uniform and non-uniform heat flux boundary for this study is presented in Fig. 1(a). The tube has a 62 mm inner diameter, a 52 mm wall thickness and a thermal conductivity of 16.27 W/mK. The tube was divided into $M \times N$ number of sections in the axial and circumferential directions. Figs.1 (b) and (c) is the cross-section of the tube model with uniform and non-uniform heat flux boundary, under the influence of gravitational field (g).

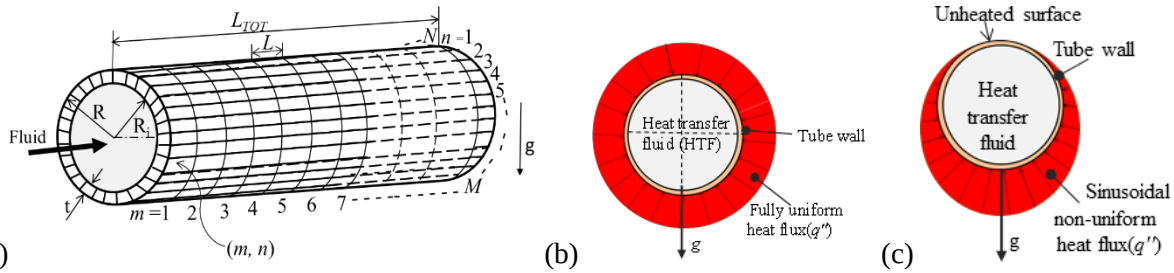

(a) (b) (c)

Fig.1 (a) Tube model in a horizontal orientation, (b) and (c) are cross-section of the tube model with uniform and non-uniform heat flux boundary.

Based on the energy balance principle applied on the element in Fig.1 (a), Eq. 1 can be obtained for steady-state conditions:

$$q_{o,(m,n)} = q_{i,(m,n)} + q_{x,(m,n)} + q_{x,(m+1,n)} + q_{\phi,(m,n)} + q_{\phi,(m,n+1)} + q_{o,conv,(m,n)} + q_{o,rad,(m,n)} \quad 1$$

$q_{o,(m,n)}$ is the incident heat transfer rate on the outer wall surface at location (m, n) expressed in Eq. (1) as follows:

$$q_{o,(m,n)} = q''_{o,(m,n)} A_{o,(m,n)} \quad 2$$

While $q_{i,(m,n)}$ is the heat transfer rate to the working fluid at location (m, n) which can be expressed as follows:

$$q_{i,(m,n)} = h_{i,(m,n)} . A_{i,(m,n)} (T_{w,i,(m,n)} - T_{b,m}) \quad 3$$

where $h_{i(m,n)}$ is the local internal heat transfer coefficient, $A_{i,(m,n)}$ is the inner wall surface area, $T_{wi,(m,n)}$ is the inner wall temperature and $T_{b,m}$ is the fluid bulk temperature at the axial position m defined as:

$$T_{b,m} = T_{b,m-1} + \frac{\sum_{n=1}^{N} q_{i,(m,n)}}{\dot{m} c_P}$$

Where m is the mass flow rate of the heat transfer fluid, c_P is the specific heat of the heat transfer fluid and $T_{b,m-1}$ is the upstream local bulk fluid temperature. The average internal heat transfer coefficient $\overline{h}_{i,m}$ is related to the average Nusselt number as follows:

International Research Journal of Applied Sciences, Engineering and Technology
Vol.8, No. 12, December-2022;
ISSN (1573-1405);
p –ISSN 0920-5691
Impact factor: 4.33

$$\overline{Nu}_{i,m} = \frac{\bar{h}_{i,m} D_i}{k_f}$$

where $\bar{h}_{i,m}$ is the circumferential average internal heat transfer coefficient at location *m*:

$$\bar{h}_{i,m} = \frac{\sum_{n=1}^{N} q_{i,(m,n)}}{\pi D_i L\left(\bar{T}_{w,i,m} - T_{b,m}\right)} \quad 6$$

and where $\bar{T}_{w,i,m}$ is the circumferential average local inner-wall temperature at location *m*:

$$\bar{T}_{w,i,m} = \frac{1}{N} \sum_{n=1}^{N} T_{w,i,(m,n)} \quad 7$$

The average internal heat transfer coefficient, $\bar{h}_i$ over the full length of the tube model in terms of the overall inner-wall surface temperature, $\bar{T}_{w,i}$ can be expressed as follows:

$$\bar{h}_i = \frac{\sum_{m=1}^{M}\sum_{n=1}^{N} q_{i,(m,n)}}{\pi D_i L_{TOT}\left(\bar{T}_{w,i} - \bar{T}_b\right)} \quad 8$$

$q_{x,(m,n)}$ and $q_{x,(m+1,n)}$ are the conductive heat transfers in the axial direction, modelled from Fourier's law of heat conduction [10]. Also, the conductive heat transfers in the tangential direction, $q_{\phi,(m,n)}$ and $q_{\phi,(m,n+1)}$ are also modelled with the Fourier law. $q_{o,conv,(m,n)}$ is the forced-convective heat transfer loss from the outer-wall surface at (*m, n*) to the surrounding of the tube modeled from Newton's law of cooling[11]. $q_{o,rad,(m,n)}$, represents the first order radiative heat transfer loss to the surrounding modelled from the Stefan-Boltzmann law of the emissive power of a surface at a thermodynamic temperature[12].

The average inner-wall heat flux ($\bar{q}''$), internal heat transfer coefficient ($\bar{h}_i$) and inner-wall-to-fluid bulk temperature difference $(\bar{T}_{wi} - T_b)$ of the absorber tube model are determined by performing numerical simulations implemented in ANSYS Fluent version 14.0 [8], under circumferential uniform heat flux and sinusoidal non-uniform heat flux distribution models. The average internal and axial local transfer coefficients were determined for the sinusoidal circumferential non-uniform heat flux distribution span of 160°, 180°, 200° and 240°, and a 360° span of circumferential uniform heat flux and the Reynolds number range of 2 600 and 100 000 based on the fluid inlet temperature.

3. Numerical simulation and model validation

The numerical simulation procedure and model validation were presented in part one. The physical properties of the absorber tube model, heat transfer fluid, solar heat flux and collector reflector parameters used in the numerical simulation are presented in tables 1 and 2. The thermal properties of the heat transfer fluid and the absorber tube material were assumed to be constant.

Property	**heat transfer fluid (water)**	**steel absorber tube**
Density [kg/m^3]	998.2	8030
Specific heat capacity [J/kgK]	4182	502.48
Thermal conductivity [W/mK]	0.61	16.27
Viscosity (μ) [N s/m^2]	0.001003	-
HTF inlet temperature [K]	300	-
Emissivity of the absorber tube [-]	-	0.85

Table 1. Properties of the heat transfer fluid and absorber tube material

International Research Journal of Applied Sciences, Engineering and Technology
Vol.8, No. 12, December-2022;
ISSN (1573-1405);
p –ISSN 0920-5691
Impact factor: 4.33

concentrator ratio, [-]	**tube absorptivity [-]**	**shape factor,[-]**	**mirror reflectivity, [-]**	**beam solar heat flux , q''_{DNI} [W/m^2]**	**concentrated solar heat flux, $q''_{w(m,n)}$ [W/m^2]**
10	0.90	1	1	787.263	7,085.367
20	0.90	1	1	787.263	14, 170.734
30	0.90	1	1	787.263	21,256.101

Table 2. Solar heat flux and concentrating collector parameters

4. Results and discussion

4.1. Temperature contours of the uniform and non-uniform heat flux distributions

Fig. 2 shows the temperature contours of the circumferential uniform heat flux and the sinusoidal circumferential non-uniform heat flux distributions of the heat flux in table 2 with C_R = 10 on the outer-wall surface of 10 m long absorber tubes. The heat transfer fluid flows through absorber tubes are in the *z*-axial direction. The temperature contours for the 360° span of uniform heat flux distribution indicated that the outer-wall temperature of the tube increased in the fluid flow direction and was greater at the outlet of the tube. The temperature contours for the 160°, 180°, 200° and 240° span of non-uniform heat flux distribution cases indicated non-uniform circumferential temperature profiles on the outer-wall surface of the tubes, which increased in the fluid flow direction and decreased tangentially from the irradiated bottom portion to the unirradiated top portion of the tubes. The contours also showed that the circumferential outer-wall temperature of the tubes was greater at the outlet of the tubes and increased with the increase in angle span of the heat flux distributions on the outer-wall surface of the tubes. The blue colour indicator at the unirradiated top portion of the tube inlet shows that the fluid layers at that portion were unheated, while the bottom portion of the tube outlet was the most heated portion of the tubes as indicated by the red hot colour. Fig. 3 shows the total surface heat flux contours for uniform and non-uniform heat flux distributions.

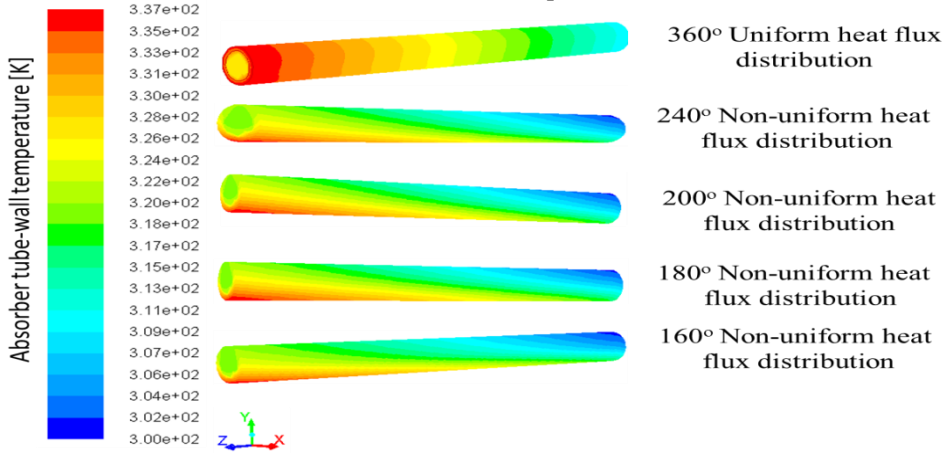

International Research Journal of Applied Sciences, Engineering and Technology
Vol.8, No. 12, December-2022;
ISSN (1573-1405);
p –ISSN 0920-5691
Impact factor: 4.33

Fig. 2 Temperature contours for uniform and non-uniform heat flux distributions

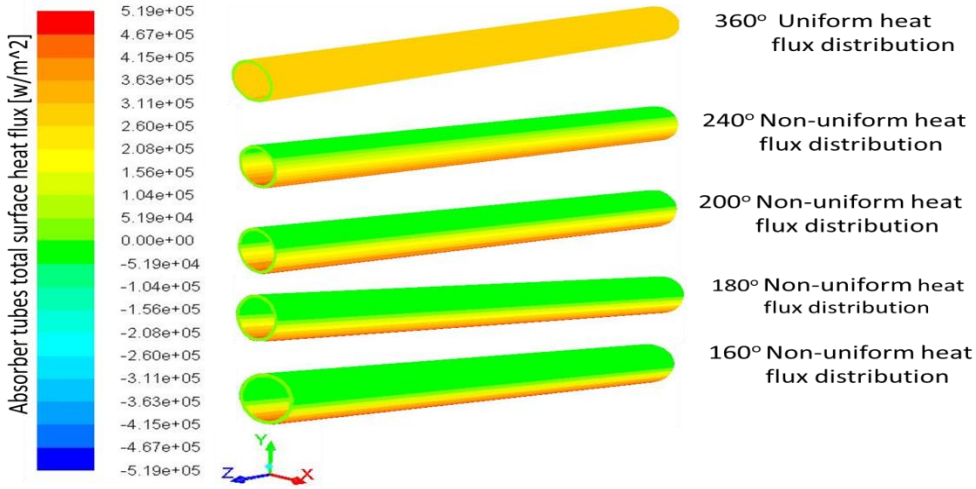

Fig. 3. Total surface heat flux contours for uniform and non-uniform heat flux distributions

4.2 Sinusoidal circumferential non-uniform heat flux distribution profiles

Fig. 4 shows the sinusoidal circumferential heat flux distribution profiles of the 160º, 180º, 200º, 220º and 240º span of the heat flux in table 2 on the outer-wall surface of the absorber tube model. It shows the peak portion of the profile, where n = 18 and 19, which corresponds to the lower central portion of the tube with the highest proportion of the heat flux distributions and the two horizontal ends of the profile, which are the unirradiated portion of the tube, where $q''_{DNI} = 0$. The sinusoidal heat flux distribution profile is similar to that of ray-tracing simulation results reported by Häberle *et al.* [1] on the optical performance of the Solarmundo line-focusing Fresnel collector using ray-tracing. The ray-tracing results showed that the solar flux radiation was evenly distributed (between 80% and 100%) at the bottom lower part and very low in the upper part of the absorber tube. The sinusoidal heat flux distributions gave an average of 97% of the radiation heat flux distributions at the lower bottom portion of the tube, where n = 18 and 19, and decreased down the unirradiated upper portion of the tube.

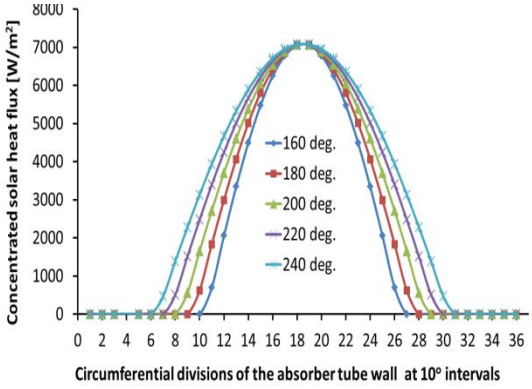

Fig. 4. Sinusoidal circumferential heat flux distribution profile

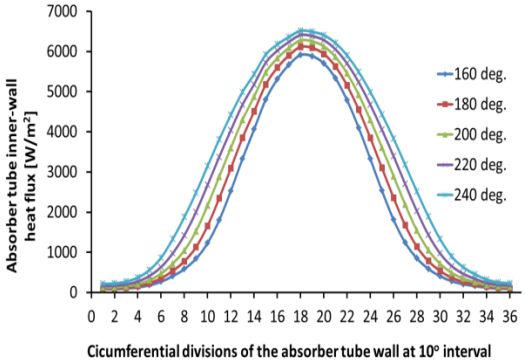

Fig. 5. Non-uniform circumferential inner- wall heat flux distribution profiles

Fig. 5 shows the circumferential inner-wall heat flux distribution profiles for five external circumferential non-uniform heat flux distributions with spans of 160º, 180º, 200º, 220º and 240º based on the sinusoidal function of the heat flux given in Fig 4. The absorber tube had an inner diameter of 0.062 m, wall thickness of 0.0052 m and thermal conductivity of 16.27 W/mK. It shows that the circumferential inner-wall heat flux value increased as the angle span of the heat flux distribution increased. It also shows that the circumferential inner-wall heat flux distribution was greatest at the peak portion of the profile. This portion corresponds to the

International Research Journal of Applied Sciences, Engineering and Technology
Vol.8, No. 12, December-2022;
ISSN (1573-1405);
p –ISSN 0920-5691
Impact factor: 4.33

lower central portion of the tube, which received the highest proportion of the incident-concentrated solar heat flux and the highest heat transfer rate to the fluid. Even though the tangential heat conduction in the tube wall resulted in the increase in the inner-wall surface heat flux at the unirradiated upper portion of the tube, the heat transfer to the fluid in these regions was still significantly smaller than at the lower portion of the tube.

4.3 Heat transfer coefficients for the absorber tubes with uniform heat flux distributions

Fig. 6 presents the variation of the average internal heat transfer coefficient with the Reynolds number for three absorber tubes of 10 m long with the same inner diameter of 62.7 mm, wall thickness of 52 mm and thermal conductivity of 16.27 W/mK. The absorber tubes were modelled with a 360° span of circumferential uniform heat flux distributions of 7.1 kW/m^2, 14.2 kW/m^2 and 21.3 kW/m^2 respectively. It was found that the average internal heat transfer coefficients of the tubes increased with the Reynolds number due to the decrease in the inner-wall-to-fluid bulk temperature difference with the Reynolds number as shown in Fig. 7. Also, the increase in the concentration ratio of the heat flux in table 2 did not result in any significant increase in the average internal heat transfer coefficient of the tubes. This shows that the average internal heat transfer coefficient was not affected by increasing the concentration ratio of the external wall heat flux distribution. However, increasing the concentration ratio of the irradiation heat flux incident on the tubes resulted in the increase in outlet temperature of the heat transfer fluid. The outlet temperature of the heat transfer fluid of the absorber tube with the heat flux of 21.3 kW/m^2 was higher than that of the absorber tube with the heat flux of 14.2 kW/m^2 by 2.5% and that of the absorber tube with the heat flux of 7.1 kW/m^2 by 5.0% between the Reynolds number range of 2 600 and 100 000.

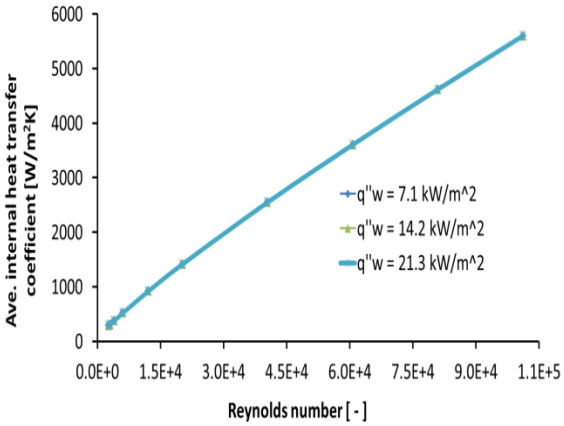

Fig. 6 Average internal heat transfer Coefficient for 360° span of circumferential uniform heat flux distributions

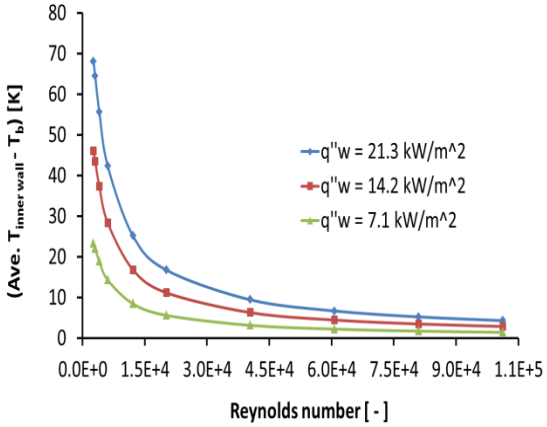

Fig. 7. Averaged inner wall–to–fluid bulk temperature difference ($T_{inner\ wall} - T_b$) with the Reynolds number

4.4 Heat transfer coefficient for the absorber tubes with different heat flux distributions

Fig. 8 shows the variation of the average internal heat transfer coefficient with the Reynolds number for five circumferential heat flux distribution cases considered.

International Research Journal of Applied Sciences, Engineering and Technology
Vol.8, No. 12, December-2022;
ISSN (1573-1405);
p –ISSN 0920-5691
Impact factor: 4.33

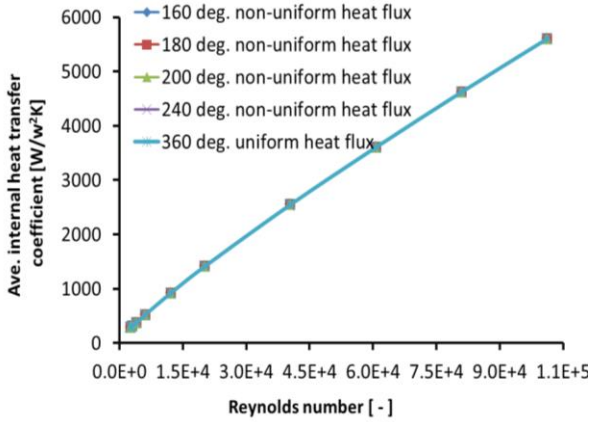

Fig. 8. Average internal heat transfer circumferential uniform and non-uniform heat flux distributions

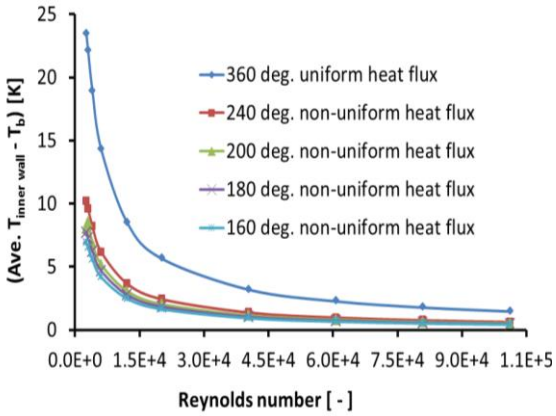

Fig. 9. Inner-wall– to–fluid bulk temp. coefficient for difference circumferential uniform and non-uniform heat flux distributions

For the 360° span case, circumferential uniform heat flux of q''_{DNI} in table 2 with C_R =10 was used, while the sinusoidal function of q''_{DNI} was also used for the case of the 160°, 180°, 200° and 240° span of circumferential non-uniform heat flux respectively. The average internal heat transfer coefficients for the circumferential uniform heat flux and non-uniform heat flux distributions increased with the increase in Reynolds number due to the decrease in the inner-wall-to-fluid bulk temperature difference and the heat flux losses. The average internal heat transfer coefficient for the absorber tube modelled with the 360° span of circumferential uniform heat flux compared with that of the absorber tubes modelled with the 160°, 180°, 200° and 240° span of non-uniform heat flux distributions is approximately the same. This indicates that, for the Reynolds number range considered in this study, the effective (average) internal heat transfer coefficient is not affected by the exterior heat flux distribution, and that the traditional heat transfer correlations could be used without modification to account for circumferential wall temperature variations.

Fig. 9 shows the variation of the inner-wall-to-fluid bulk temperature difference with the Reynolds number for the heat flux cases in Fig. 8. The average inner-wall-to-fluid bulk temperature difference for the absorber tube modelled with the 360° span of uniform heat flux where C_R = 10 was 57%, 64%, 67% and 71% higher than that of the absorber tubes modelled with 240°, 200°, 180°, and 160° spans respectively for an effective average heat flux of 4.5 kW/m^2. The inner-wall-to-bulk temperature difference is inversely related with heat transfer coefficient and directly related to the heat flux losses, which indicates that the heat transfer coefficient increases with the decrease in the inner-wall-to-bulk temperature difference and heat flux losses and increases with the Reynolds number. The increase in the internal heat transfer coefficient with the Reynolds number is more influenced by the decrease in the inner-wall-to-fluid bulk temperature difference than that of the decrease in heat flux loss. However, the physical mechanism behind this could actually be due to the turbulent nature of the fluid particles with the increase in Reynolds number.

The circumferential internal heat transfer coefficient of the absorber tube, which is a function of the circumferential inner-wall heat flux of the tube and the circumferential inner-wall-to-fluid bulk temperature difference, also varied along the circumferential inner-wall surface of the tube. At the unirradiated portion of the tube where the inner-wall-to-fluid bulk temperature difference is negative, it also resulted in the negative heat transfer coefficient, which indicates that the tube is losing heat from the unirradiated portion and therefore required to be insulated.

The axial local internal heat transfer coefficient was found to decrease with an increase along the length of the tube. The axial local internal heat transfer coefficient for the absorber tube modelled with a 360° span of uniform heat flux for the case where C_R = 10 was 0.64%, 0.61% and 0.53% higher than that of the absorber tubes modelled with the 160°, 200° and 240° span of circumferentially averaged non-uniform heat flux distributions respectively.

International Research Journal of Applied Sciences, Engineering and Technology
Vol.8, No. 12, December-2022;
ISSN (1573-1405);
p –ISSN 0920-5691
Impact factor: 4.33

4.5 Heat transfer coefficient for absorber tubes with different inner diameters and wall thicknesses

The average internal heat transfer coefficient for four absorber tubes with different inner diameters and wall thicknesses, with thermal conductivity of 16.27 W/mK and modelled with a 200° span of the sinusoidal function of the flux in table 2 with C_R = 10 were investigated. It was found that the average internal heat transfer coefficient of the tubes increased with the increase in mass flow rate of the heat transfer fluid and also increased with the decrease in the inner diameter and wall thickness of the tube. The average internal heat transfer coefficient for the absorber tube with a 35.1 mm inner diameter and 3.56mm wall thickness was 24.74% , higher than that of the absorber tube with a 40.9 mm inner diameter and a 3.68 mm wall thickness, 52.79% higher than that of the absorber tube with a 52.5 mm inner diameter and a 3.91 mm wall thickness, and 65.97% higher than that of the absorber tube with a 62.7 mm inner diameter and a 5.16 mm wall thickness between the mass flow rate of 0.15 kg/s and 10 kg/s. It implied that the inner diameter and wall thickness of an absorber tube and mass flow rate of the heat transfer fluid have very important effects on the internal heat transfer coefficient of the tube. However, decreasing the absorber tube inner diameter to enhance the internal heat transfer coefficient would result in an increase in pressure drop, since pressure is inversely related to the tube diameter.

The pressure drops for the absorber tubes were obtained from the numerical results. The pressure drop of the absorber tube with a 35.1 mm inner diameter was 52% higher than that of the absorber tube with a 40.9 mm inner diameter, 85% higher than that of the absorber tube with a 52.5 mm inner diameter and 93% higher than that of the absorber tube with a 62.7 mm inner diameter. It was found that the pumping power required to sustain the fluid flow and heat transfer to the fluid for the absorber tube with a 35.1 mm inner diameter was 58.67 % higher than that of the absorber tube with 40.9 mm inner diameter, 90.22 % higher than that of the absorber tube with a 52.5 mm inner diameter and 96.49 % higher than that of the absorber tube with a 62.7 mm inner diameter. This implies that the increase in pumping power as a result of higher pressure drop with decrease in tube inner diameter would be a limiting factor to increasing the internal heat transfer coefficient of a trapezoidal cavity receiver of a linear Fresnel collector which uses multiple absorber tubes of small diameter, since increase in pumping power required to overcome the pressure drop of the tubes would lower net power output of the system.

5. Conclusion

This study has numerically investigated the heat transfer performance of a linear Fresnel solar collector absorber tubes with circumferential uniform heat flux and sinusoidal non-uniform heat flux under steady-state and turbulent flow conditions. In both cases of the heat flux distributions, the average internal heat transfer coefficient for the absorber tubes considered increased with the increase in Reynolds number. It was found that the average internal heat transfer performance for the circumferential uniform heat flux with different concentration ratios were approximately the same. It was also found that the average internal heat transfer performance for the circumferential uniform heat flux compared with that of the sinusoidal circumferential non-uniform heat flux distributions on the absorber tube of the same inner diameter, wall thickness and thermal conductivity, was approximately the same as that of the non-uniform heat flux distribution cases of a lower average heat flux than that of the circumferential uniform heat flux. This shows that the average internal heat transfer performance of the absorber tubes was not affected by the exterior heat flux distribution. The average internal heat transfer coefficient was found to increase with the decrease in the inner diameter and the wall thickness of the absorber tubes of the same thermal conductivity.

References

A. Häberle, C. Zahler, H. Lerchenmüller, M.Mertins, C.Wittwer, F.Trieb, and J.Dersch. The Solarmundo line focussing Fresnel collector: Optical and thermal performance and cost calculations. Fraunhofer Institute for Solar Energy Systems, Heidenhofstr. 2, 79110 Freiburg, Germany.

R.P.Goswami, B.S. Negi, H.K. Sehgal, and G.D. Sootha. Optical Designs and Concentration Characteristics of a Linear Fresnel Reflector Solar Concentrator with a Triangular absorber. Solar Energy Materials 1990; 21: 237-251.

S. S. Mathur , T. C. Kandpal and B. S. Negi. Optical Design and Concentration Characteristics of Linear Fresnel Reflector Solar Concentrators-

II. Mirror Elements of Equal Width. Energy Convers. Mgmt 1991; 31 (3): 221-232.

C. J. Dey. Heat Transfer Aspects of an Elevated Linear Absorber. Solar Energy. 2004; 76: 243–249.

R. Abbas, J. Muñoz and J.M. Martínez-Val. Steady-State Thermal Analysis of an Innovative Receiver for Linear Fresnel Reflectors. Renewable Energy 2012; 39: 198-206.

J. Francisco, C. Rosario, R. L. Juan., R. Felipe, and G. José. Exp. Validation of an Optical and Thermal Model of a Linear Fresnel Collector 2nd European Conf. on Polygeneration – Tarragona, Spain: 1- 8: 2011.

N. Velázquez , O.García-Valladares, D. Sauceda and R.Beltrán. Numerical simulation of a Linear Fresnel Reflector Concentrator as Direct Generator in a Solar-GAX cycle. Energy Con. and Mgt. 2010; 51: 434–445.

ANSYS Fluent version 14.0 Users' Guide ANSYS, Release 14.0 Incorporated, Southpointe 275 Technology Drive Canonsburg, PA 15317.

J. H. Ferziger and M. Perifi. Computational Methods for Fluid Dynamics, 3 Rev. ed.- Berlin; Heidelberg; Hong Kong; London; Milan; Paris; Tokyo: Springer, 2002.

Y. A. Cengel, Heat and Mass Transfer: A Practical Approach, Published by McGraw Hill Companies, Inc. 1221 Avenue of the Americas, New York, NY 10020; 3rd Edition, 2007.

R. K. Rajput, Heat and Mass Transfer in SI Units. Second Edition, Published by S. Chand and Company Ltd, Ram Nagar, New Delhi, 110 055, 2005.

J. Hameury, B. Hay and J-R. Filtz, Measurement of Total Hemispherical Emissivity Using a Calorimetric Technique, Laboratoire National de Métrologie d'Essais (LNE), 29 Avenue Roger Hennequin, 78197 TRAPPES Cedex, France,(2005) 1-14